D.4.9 – Long term storages operation and performance

Renewable and Waste Heat Recovery for Competitive District Heating and Cooling Networks

REWARDHeat

Project Title: Renewable and Waste Heat Recovery for Competitive District Heating and Cooling Networks

Project Acronym: REWARDHeat

Deliverable Title: Long term storages operation and performance

Lead beneficiary: EURAC

Amir M. Jodeiri, EURAC

Francesco Turrin, EURAC

Christian Keim, EDF

Caroline Laget, DALKIA

Aurelien Galmiche, DALKIA

Due date: 31 December 2023(due)

QUALITY CONTROL ASSESSMENT SHEET			
Issue	Date	Comment	Author
V0.1	05.08.2024	First draft sent to reviewers	Christian Keim – EDF
V0.2	04.10.2024	Second draft sent to reviewers	Amir M. Jodeiri
V0.3	15.10.2024	Third draft sent to reviewers	Francesco Turrin
V1.0	18.10.2024	Submission to the EC	Roberto Fedrizzi

This document has been produced in the context of the REWARDHeat Project.

This project has received funding from the European Union's Horizon 2020 research and innovation programme under grant agreement No. 857811. The European Commission has no liability for any use that may be made of the information it contains

Table of Contents

1 Introduction 1

2 Gardanne mine shaft as a storage 2

2.1 Mine shaft as a storage – problem formulation 3

2.2 Mine shaft as storage – Analysis 5

2.3 Conclusions 11

3 Helsingborg BTES as a storage 13

3.1 BTES system 13

3.2 BTES model 16

3.3 One-year BTES simulation with and without DH 20

3.4 10-year BTES simulation with and without DH 25

3.5 Conclusions 27

4 Overall Conclusions 29

5 References 30

List of acronyms

API	Application Programming Interface
BESS	Battery Energy Storage Systems
COP	Coefficient of Performance
DHCN	District Heating and Cooling Network
HP	Heat Pump
LT	Low Temperature
PDS	Public Delegation of Service
PV	Photovoltaics
RES	Renewable Energy Sources
REX	Return of experience
SUB	Substation
BTES	Borehole Thermal Energy Storage
DH	District Heating
GSHP	Ground Source Heat Pump
HX	Heat Exchanger
MFR	Mass Flow Rate
PVT	Photovoltaic-Thermal
RMSE	Root Mean Squared Error

List of symbols

$\dot{m}_{BTES}$	Mass flow rate to/from BTES (kg/h)
$T_{in,BTES}$	Inflow Temperature to BTES (°C)
$T_{out,BTES}$	Outflow Temperature from BTES (°C)

1 Introduction

The REWARDHeat project aims to revolutionize district heating and cooling networks by integrating renewable and waste heat recovery technologies. This deliverable, D4.9, focuses on the long-term operation and performance of thermal energy storage systems, specifically the Gardanne mine shaft and the Helsingborg Borehole Thermal Energy Storage (BTES) system.

Chapter 2 of this report delves into the Gardanne mine shaft, a historic coal mine repurposed as a thermal energy storage solution. Located in Gardanne, France, this mine shaft is the largest in Europe, measuring 1,100 meters deep and 10 meters in diameter. The study explores the potential of the mine shaft to serve as a seasonal storage system, leveraging its large water volume and depth to balance the DHCN's energy demands. The analysis includes temperature data collection, numerical simulations, and the development of an optimized operational strategy.

Chapter 3 examines the Helsingborg BTES system, which integrates geothermal energy with district heating and cooling. Located in the Infanteriet neighborhood of Helsingborg, Sweden, this system consists of a borehole field that serves as a geothermal source and is partially recharged using thermal energy from photovoltaic-thermal (PVT) collectors and rejected heat from space cooling systems. The chapter presents a detailed simulation model to evaluate the system's performance over short and long-term periods. The analysis compares scenarios with and without district heating energy use to directly charge the BTES, assessing the impact on energy costs and system thermal balance.

2 Gardanne mine shaft as a storage

Located in the town of Gardanne, this historic coal mine, operated from 1989 to 2003, is the largest mining shaft in Europe, measuring 1,100 meters deep and 10 meters in diameter. Currently filled with water, it plays a vital role in ensuring the geological stability of the terrain. The site is under partial construction with several operational real estate projects dedicated to tertiary activities, aiming for an 80,000 m² total upon completion. The area is served by a district heating and cooling network (DHCN), which uses the mineshaft as the primary balancing source.

As shown in the figure below, the DHCN system operates as follows:

- Water is extracted via a dedicated DN 100 extraction pipe from a depth of -333m. The mine is not fully filled with water but is maintained at a constant depth of -259m through third-party pumping operations.
- A single pump transports the water to the top of the shaft, where it flows through a heat exchanger to balance the DHCN's primary circuit.
- After passing through the exchanger, the water is re-injected into the mine at a depth of -958m through another DN 100 pipe.

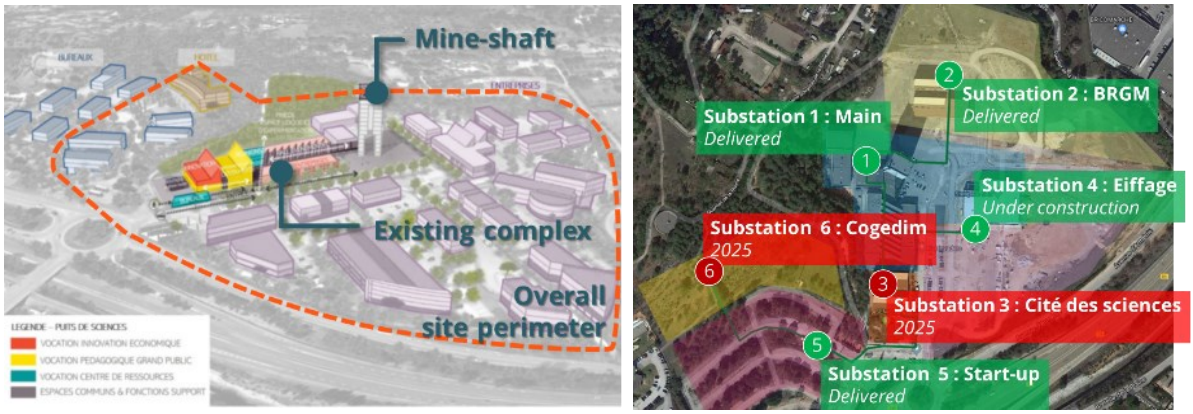

Figure 1: bird's-eye view of the site, identifying the former mine location and the DHCN perimeter. The green areas represent substations currently operational or under commissioning, while red indicates those delayed (Source: EDF).

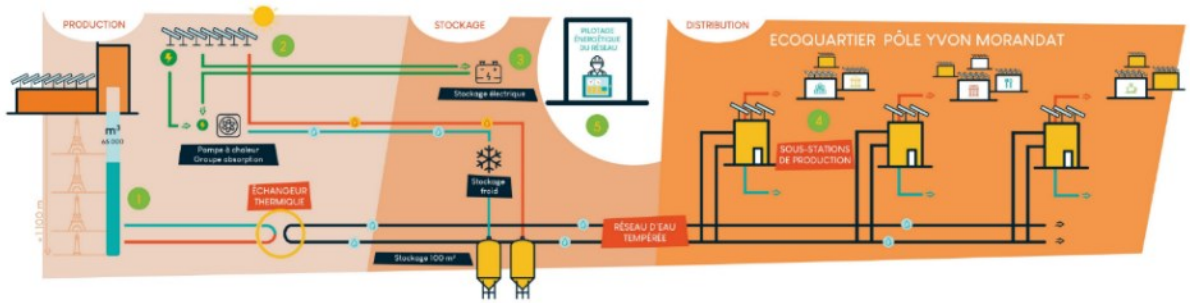

Figure 2 : schematisation of the site's working principle, integrating the thermal and electric smart grids (Source: DALKIA).

The mineshaft is equipped with advanced fiber-optic sensors from top to bottom, enabling the collection of temperature data along the entire 1 km shaft. At present, the DHCN uses the well solely as a balancing source, without optimizing the withdrawal or injection to leverage the storage capacity of the 65,000 m^3 of water in the shaft.

The aim of the study presented in this report is to leverage the data and knowledge gathered on the well's behaviour to develop an optimized operational strategy for the DHCN, utilizing the well as a seasonal thermal energy storage solution.

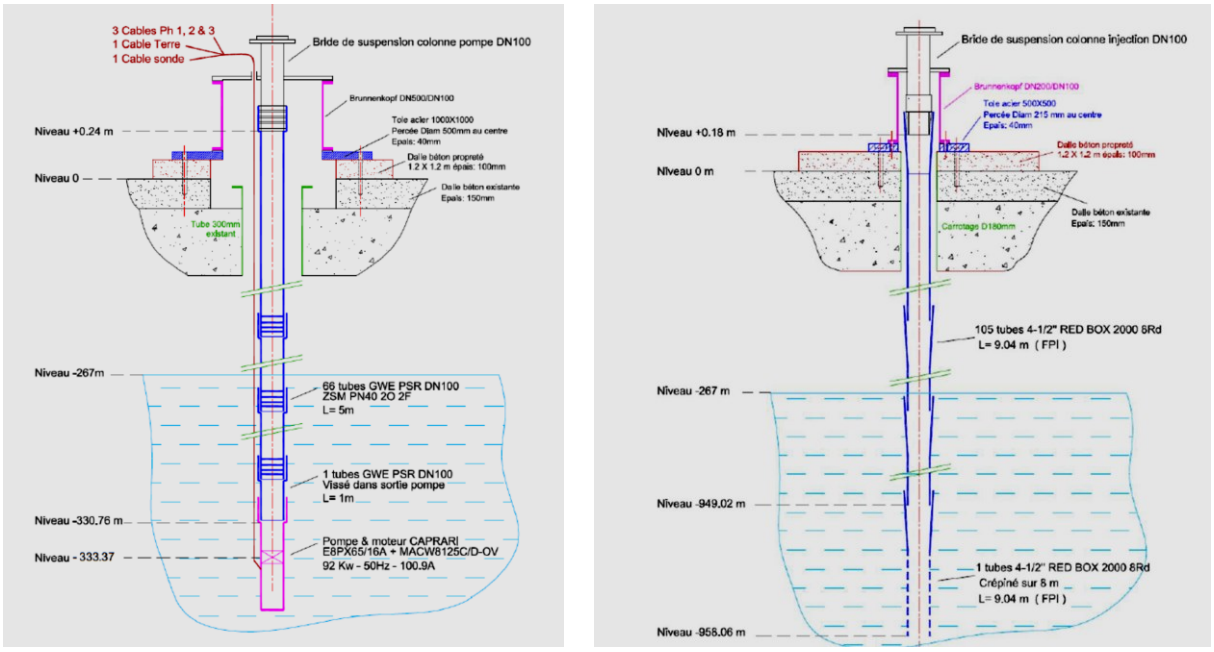

Figure 3 : section-view of the extraction (left) and injection (right) of the balancing source circuit (Source: BRGM).

2.1 Mine shaft as a storage – problem formulation

Initial analyses and calculations performed by DALKIA (shown in Figure 4) indicated that the well could potentially serve as a mid-term or seasonal storage solution between winter and summer, improving the DHCN's overall performance. The original assumption during the design and sizing phase of the DHCN was that the mineshaft functioned as a closed system, which was also the assumption when the public authority launched the project.

In the first assessment phase, temperature data from various depths over several years were collected and analysed alongside the energy extracted and injected by the DHCN. This revealed that the well's temperature was disconnected from DHCN operations, suggesting that an exogenous factor might be the primary determinant of the well's temperature. This unexpected finding prompted the need for a more in-depth analysis to better understand the well's behaviour.

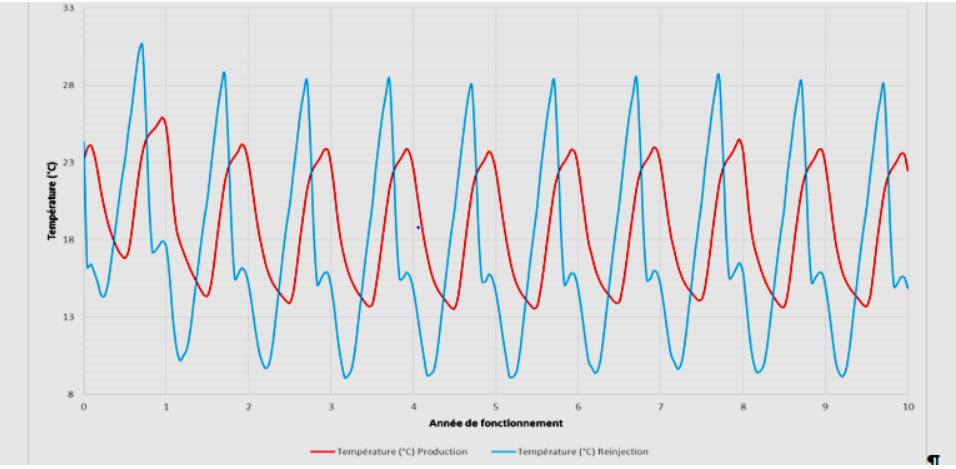

Figure 4: Numerical simulation of inlet and outlet temperatures in the well during 10 years > seasonal temperatures variation indicates an untapped potential of operational performance increase through seasonal injection/extraction control (Hypothesis: semi-conductive walls); Red – water extraction temperatures; Blue – water injection temperatures (Source: DALKIA).

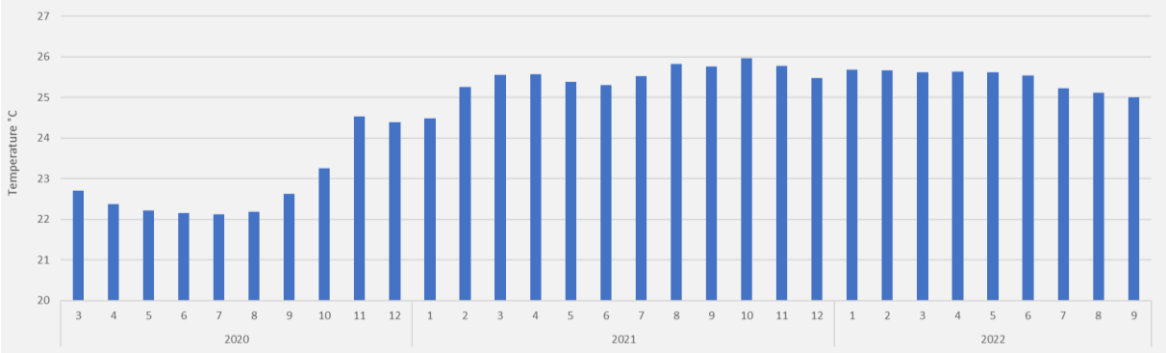

Figure 5 : Well temperature variations were monitored during several years. It is obvious that unknown phenomena, such as one or more underground flows, have a greater impact on the temperature profile than thermal loads exerted by the heat pumps (Source: DALKIA).

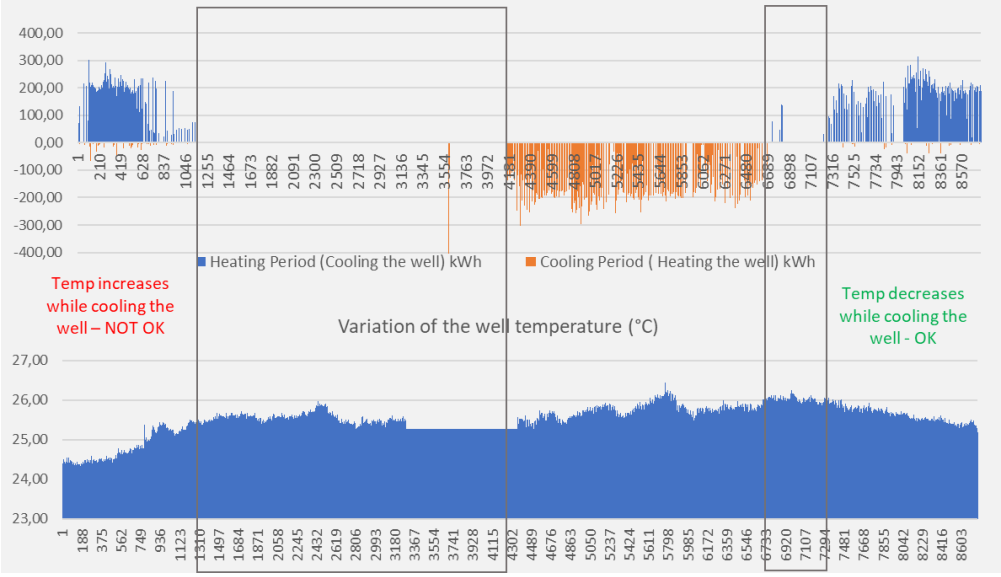

Figure 6 : Amount of energy extracted and injected into the well during 2021 in kWh. The grey squares indicate periods when the well was not functioning due to different reasons. Source: DALKIA.

In 2021, the energy extracted and injected was 145 MWh and 143 MWh, respectively, leaving the system nearly balanced, with only a 2.4 MWh offset favouring heating. Therefore, temperatures were expected to decrease, yet this was not observed. The data suggests potential influences from factors such as water movements or convection within the well.

Conversely, in subsequent years, temperatures began to rise with some fluctuations during the cooling period, decreasing during the heating period as expected. One possible explanation could be the long-term stabilization of water layers within the well after being disturbed by the DHCN's commissioning. However, the analysis remains inconclusive, and it seems likely that an external water source is affecting the network.

As a result, DALKIA decided to collaborate with BRGM, France's public reference institution for Earth science applications in surface and subsurface resource management. The Gardanne mine complex falls under BRGM's jurisdiction, making it an ideal partner to shed light on this matter. Since the end of 2023, a dedicated study has been underway with the following objectives:

a) Identify the causes of the observed well behaviour;

b) Develop a simplified model for this analysis;

c) Assess the feasibility of using the well as a storage solution or explore other operational strategies.

2.2 Mine shaft as storage – Analysis

In the first phase of the study, DALKIA's metering data was cross-referenced with additional data from the mine complex, collected by BRGM. This phase confirmed that the well (Yves Morandat well) is directly influenced by the neighbouring Gerard well and its pumping activity. Water infiltrations were also consistent, caused by an aquifer (one-third) and rainfall from surrounding valleys (two-thirds).

It is important to note that the groundwater level is kept at around -259 meters (with minor variations throughout the year), and dedicated pumping systems maintain this level to ensure the geological stability of the mine system, particularly in the Gerard well. This, combined with the water infiltrations, is the primary cause of the water movements observed in the mineshaft. For reference, the Gerard well averages a flow of 700 m^3/h over the course of the year, significantly influencing the DHCN's water source in the Yves Morandat well.

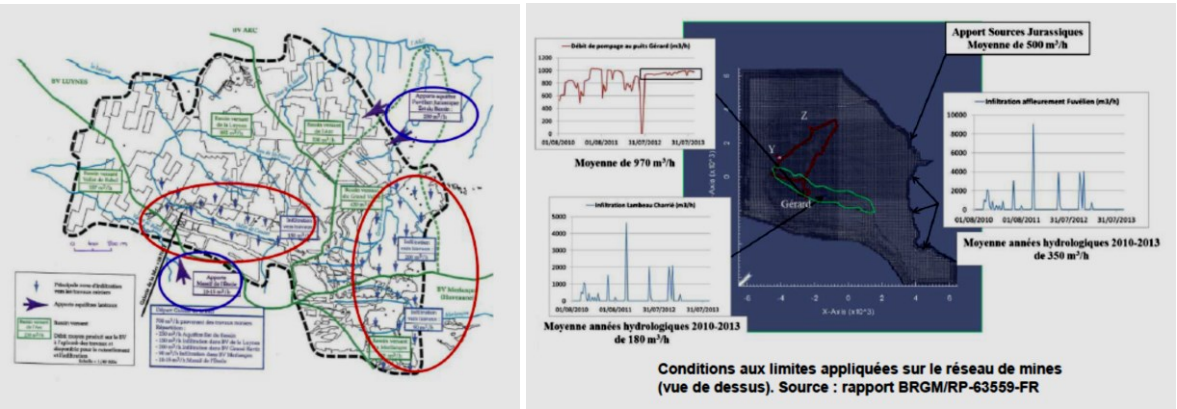

Figure 7: left - extent of the analysed mine-system in Gardanne; right – different data sources integrated for the study (Source: BRGM).

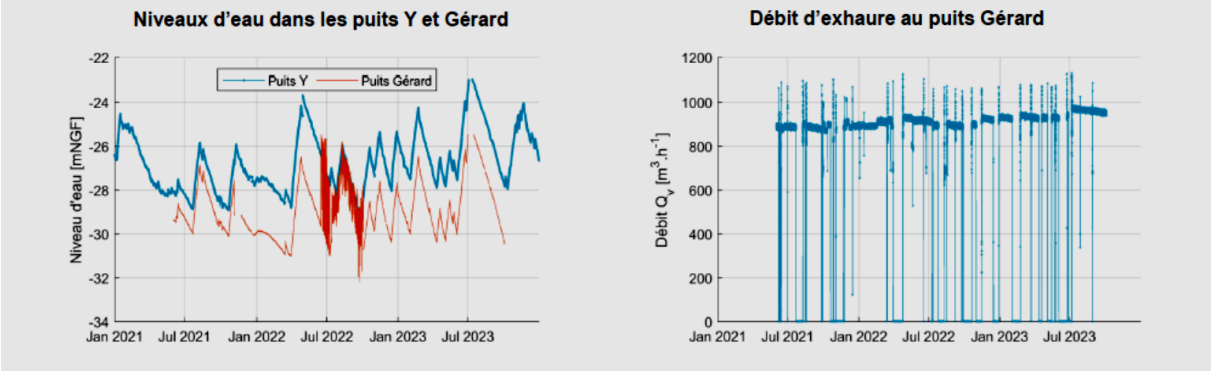

Figure 8: the site's well is under direct hydraulic influence of the Gerard well, so the out-flows from the latter (right), influences the water level in the site's well (left). Source: BRGM.

Indeed, this proves that the analysis perimeter known for the DHCN design phase lacked crucial information, resulting in an incomplete understanding of the mineshaft's behaviour. It has been established that the well operates as an open system, heavily influenced by exogenous factors. Had this information been available at the outset of the DHCN project, it could have significantly altered the design solutions and the overall approach toward utilizing the well.

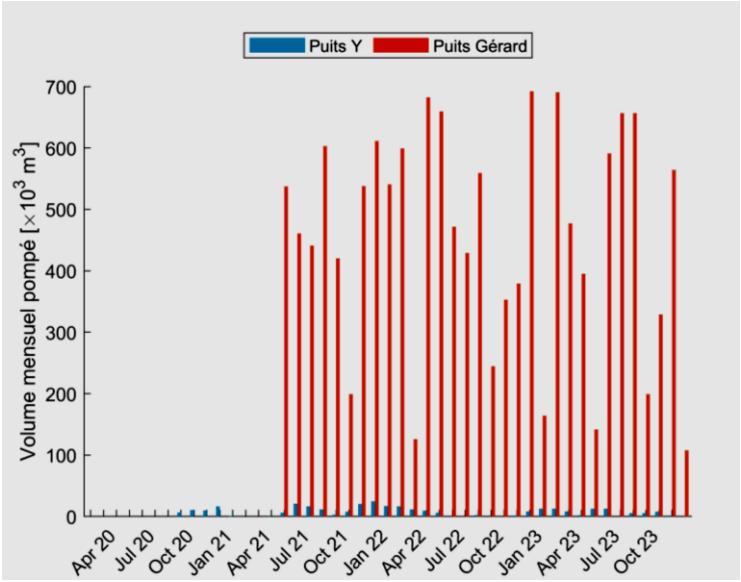

Figure 9: comparison of the monthly pumped water volumes between the DHCN in puits Y. Morandat (blue) and that of the Puit Gerard shaft (red). A rather important disparity of volume (and thus influence) can be evinced by this comparison (Source: BRGM).

These water flows affect the temperature distribution across the +700m water column in the well. The DHCN's pumping activity and related volumes influence overall electricity demand, and extraction temperatures are a key determinant of the DHCN heat pumps' coefficient of performance (COP). As a first step, BRGM's study integrated temperature data retrieved from DALKIA at various depths, enriched with additional studies and data, to assess the impact.

This analysis of long-term temperature distribution was further enriched by examining the variation in shaft temperatures in relation to DHCN pumping activities. The goal was to determine how water extraction/injection influences temperature distribution within the well.

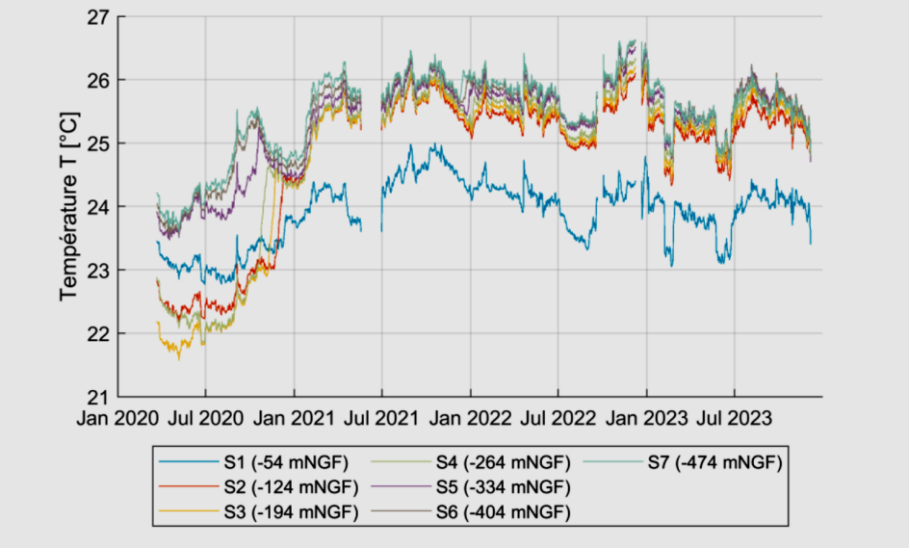

Figure 10: Visualisation of the metered temperature over several years as collected by DALKIA via the fiber optic sensors (Source: BRGM).

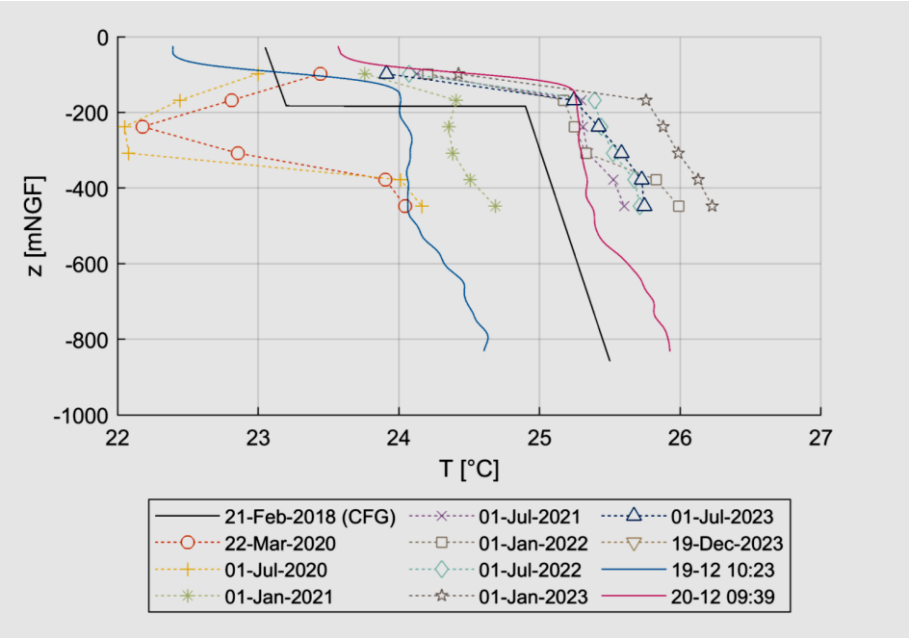

Figure 11: vertical temperature profiles of the shaft, during different seasons and years. TO notice the change in temperatures at the surface of the water column, due to the change in chemical composition of the water (Source: BRGM).

To complete the system's description, additional meteorological data (pluviometry) was collected for the same period to assess the impact of water infiltrations into the mine shaft. All of this information has been incorporated into a model developed by BRGM, which is designed to study the well's short- and long-term behaviour under varying operational or meteorological conditions.

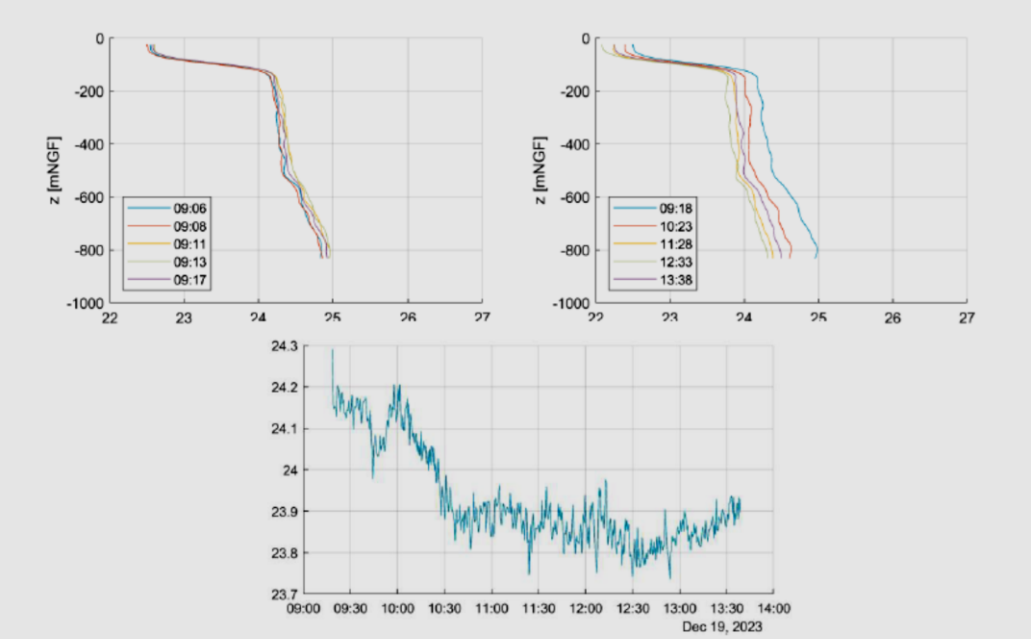

Figure 18 : Températures mesurées le 19 décembre 2023 : baseline (en haut à gauche) et pendant le fonctionnement de la pompe (en haut à droite). Température moyenne sur toute la hauteur de la fibre optique pendant le test (en bas)

Figure 12: comparison of the baseline temp. distribution (top-left) and during operation of the DHCN's pump (top-right) and the variation of the temperature of a meter during the same time-period (Source: BRGM).

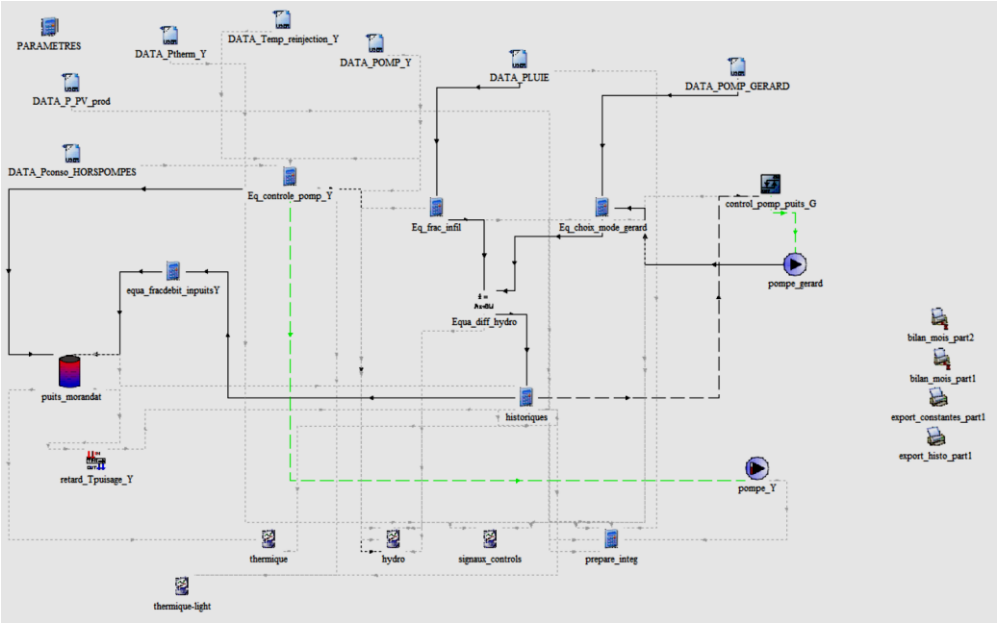

Figure 13: Screenshot of the TRNSYS model developed by BRGM (Source: BRGM).

The semi-empirical model includes several parameters calibrated against the available data. Implemented using the TRNSYS dynamic systems simulation software, TRNSYS enables the assembly and connection of various components—such as pumps, tanks, pipes, or heat exchangers—and the definition of associated control strategies. Matlab® software was employed

to prepare, format, and analyse the TRNSYS data and results, as well as to calibrate the model parameters. The model operates with a time step of 10 minutes, and a calculation server allows the simultaneous evaluation of up to 32 models. Hydraulic and thermal models of the system were developed and calibrated based on the collected data. Scenario analysis was performed to study the behaviour of three factors: flow rate, temperature, and the influence of rainfall (pluviometry) on the mineshaft.

To ensure comparability, a reference scenario was defined: the flow rate and reinjection temperature were measured from 1 January to 4 December 2023, using 2022 rainfall data. These conditions are repeated yearly, and the Gérard well pump is controlled to maintain a water level within a 2-meter range of variation. Under the reference scenario, the dynamics of the water level in the Yves Morandat well closely followed those in the Gérard well. The production temperature in the Yves Morandat well stabilized around 24°C, with variations of less than 1°C. Overall, in the reference scenario, the well was cooled by -146 MWh/a and warmed by 247 MWh/a, resulting in a total recovery of 393 MWh/a of thermal energy. Electricity consumption for pumping was 131 MWh/a, representing approximately 33% of the recovered thermal energy. This reference scenario was then compared to other scenarios, varying flow rate, injected temperature, or both, as well as water infiltration due to rainfall.

In summary, the scenarios explored include the following:

- Influence of Re-injection Temperature (at unchanged flow rate): A re-injection temperature change of ±10°C results in a production temperature change of ±1.5 to 2°C. The amount of thermal energy exchanged increases significantly with minimal impact on production temperatures. For instance, with a re-injection temperature of -10°C, the amount of cold exchanged increases from -145.8 MWh/a to -877.6 MWh/a. Symmetric behavior is observed for heating.
- Influence of Flow Rate (at unchanged reinjection temperature): Increasing the withdrawn and reinjected flow rate enhances the heat energy exchanged with the well. However, the additional heat exchange is less pronounced at higher flow values, reflecting the well's finite exchange capacity.
- Simultaneous Influence of Flow Rate and Re-injection Temperature: When both factors are varied within their respective ranges, two zones emerge where the minimum and maximum production temperatures remain unchanged from the reference scenario. The same applies to the quantities of heat and cold exchanged (see figures below).
- Finally, it is possible to simultaneously increase the reinjection temperature difference (in absolute terms) and flow rate to increase the amount of heat or cold exchanged while maintaining or even reducing the pump's energy consumption. To achieve this, the iso-value lines (e.g., "0.20" for Eel pompY* = 20%) in the figure below should be followed. However, increasing the extracted temperature in summer and decreasing it in winter will result in reduced performance for the heat pumps (HPs) connected to the tempered water loop.
- Influence of Rainfall: Over the course of a year, the volume pumped at the Gérard well closely matches the volume infiltrating the catchment area. A reduction in the volume pumped at Gérard would result in less water flowing from Gérard to the Yves Morandat well, leading to reduced water renewal in the latter. For the reference scenario (which is unbalanced toward heating over the year), this would cause a relatively small temperature increase, not exceeding +2°C, even under the hypothetical condition of several years without precipitation. This observation holds true even if the flow rate is multiplied by a factor of 3 to 5. If the well is

operated with a significantly higher heating load than in the reference scenario (ΔTreinj = +10°C) and with the flow rate increased by 5, in the absence of precipitation, the maximum production temperature would rise by 4°C compared to normal precipitation conditions.

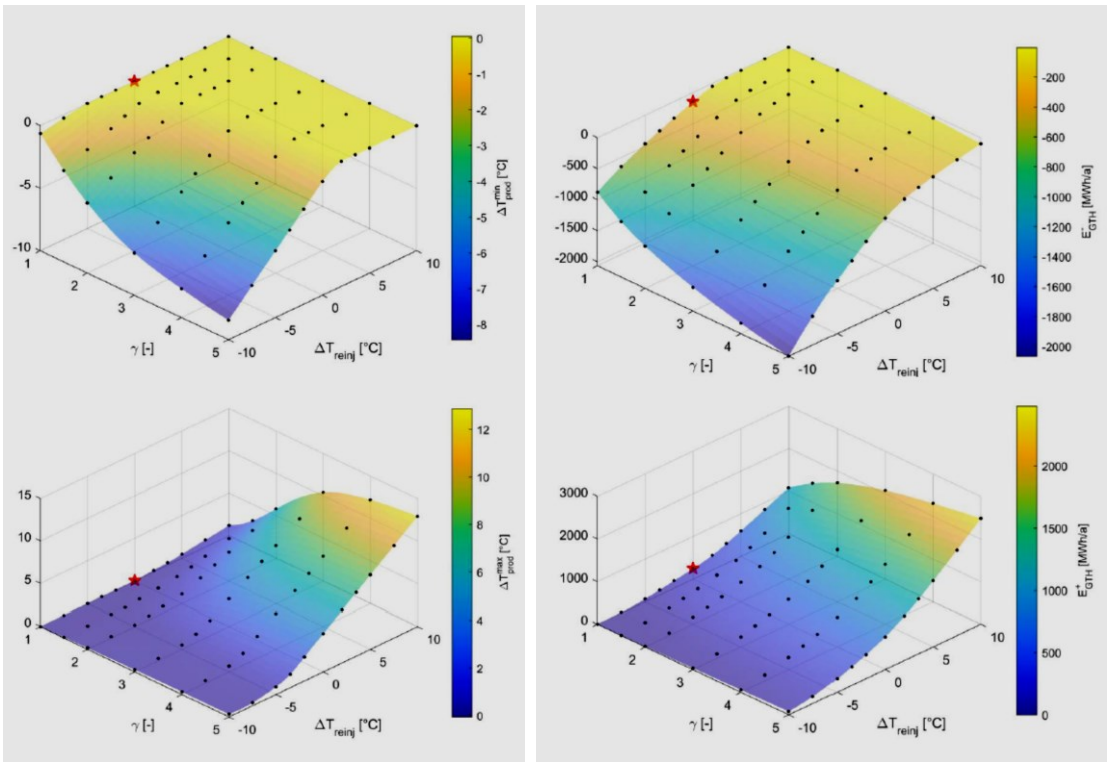

Figure 14 : on the left - Temperature deviations from the minimum (ΔTprodmin, top) and maximum (ΔTprodmax, top) reference scenarios as a function of γ and ΔTreinj; right - Quantities of cold (top) and heat (bottom) exchanged with the well as a function of γ and ΔTreinj (Source: BRGM).

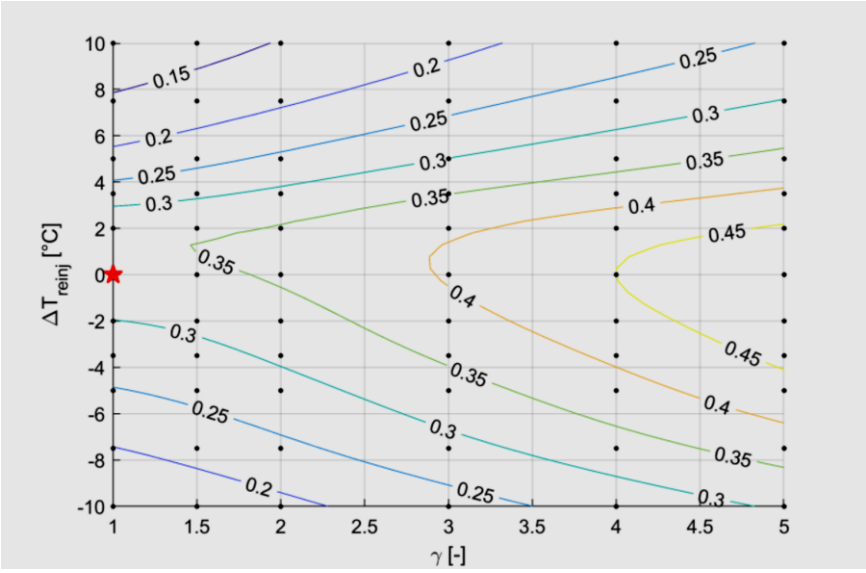

Figure 15 : Normalized consumption of well pump depending on injected temp. difference and flow (Source: BRGM).

2.3 Conclusions

A semi-empirical hydraulic and thermal model of the Yves Morandat well was developed, accounting for environmental influences such as pumping at the Gérard well and rainfall/infiltration on the water level. Once the model parameters were set, it successfully replicated changes in the water level. However, establishing the thermal model, which predicts temperature profiles within the well, was more challenging. While the model accurately reproduces the temperatures in the production zone, it requires further refinement to improve its predictions at deeper levels of the water column. In-situ water measurements did not reveal any preferential inflows into the well, which would have otherwise constrained the thermal model.

Despite these limitations, the model remains useful for studying the impact of operating flow rates and reinjection temperatures on the quantities of heat and cold exchanged, as well as the associated pump consumption. Certain combinations of flow rates and reinjection temperatures resulted in minimal changes to the production temperature when compared to 2023 conditions. Increasing the temperature difference between the extracted and injected water reduced the pump's electricity consumption relative to the amount of energy delivered by the well. However, this reduction in energy usage would slightly decrease the performance of the DHCN's heat pumps (HPs).

From a modelling perspective, the study concluded that while the model could be improved or expanded through alternative methodologies, the accuracy of the metering equipment should also be verified. Some data raised concerns, such as the lack of noticeable temperature change upon pump start-up—an indication of a stagnation effect. Normally, heat losses would be expected in the extraction pipe at start-up, but the data did not reflect such changes. Therefore, it is recommended to add additional metering equipment to verify and validate the data being collected.

From the operational point of view of the DHCN, the study suggests that in the short-to-midterm (2 to 5 years), altering the operational conditions will have little impact on the water temperature or stratification within the well. The exogenous factors, such as maintaining a constant water level at the Gérard well and the effects of water infiltration/rainfall, play a far more significant role than the DHCN's pumping activities. The aim is to explore long-term (around 10 years) operational strategies using the model to assess potential system impacts. Nonetheless, at present, no alternative operation strategies or design modifications seem capable of enabling energy storage in the mineshaft.

2.3.1 Lessons learned

- Early Feasibility Stage – Source Qualification: Through the project, a more comprehensive understanding of the mining system around the Yves Morandat shaft was achieved. The study revealed that several assumptions made at the inception of the DHCN project were inaccurate. This new knowledge may have led to alternative design solutions, potentially reducing investment costs and improving system performance (such as optimizing the sizing of the piping system for extraction/injection and associated operation modes).
- Early Feasibility Stage – Source Qualification: The operation of the DHCN has shown that the mine water is contaminated by iron-oxidizing bacteria. This contamination has led to frequent and continuous interventions on the balancing source system, requiring the cleaning, treatment, and replacement of the heat exchanger, which is particularly sensitive to this issue. Additionally, the contamination accelerates the aging of the system and increases the frequency and severity of interventions, leading to higher operational costs. The occurrence

of these issues and related interventions causes the well to shut down, making the DHCN's balancing source temporarily unavailable.

- Design Stage – Balancing Source Solution Design: As described in the introduction, the source pump has been immersed in the well. This design choice has resulted in several operational challenges. The design and operation need to consider the possibility of a "venturi effect" and incorporate solutions to address it in future schemes. However, operating and maintaining the current solution in such a difficult and potentially dangerous environment has proven problematic. For future replication of this DHCN solution, it would be preferable to locate the pump at ground level and immerse the heat exchanger in the well instead. This alternative design would reduce the risk of chemical or biological contamination of the mine water, limiting exposure to only the submerged exchanger and piping. As a result, the overall piping and pump would have a longer lifespan and require fewer interventions. Additionally, maintenance on an immersed heat exchanger would be less complex and costly than the current solution.

3 Helsingborg BTES as a storage

The Infanteriet neighborhood in Helsingborg (refer to deliverable D4.5) consists of two 5-story and two 7-story buildings, encompassing a total heated floor area of 7,795 m^2, arranged around a communal yard. As part of the REWARDHeat project, a borehole field has been established, serving as a crucial component of the standardized energy centre that seamlessly integrates district heating (DH) and geothermal energy utilization.

Currently, the borehole field functions as a geothermal source and is partially recharged using thermal energy from photovoltaic-thermal (PVT) collectors and rejected heat from space cooling systems in the buildings. The focus of the assessment presented in this section is to explore the potential for extending its use as a seasonal thermal storage solution.

Figure 16. Building blocks before implementation of construction project (Left) and render of newly constructed blocks post-implementation (Right)

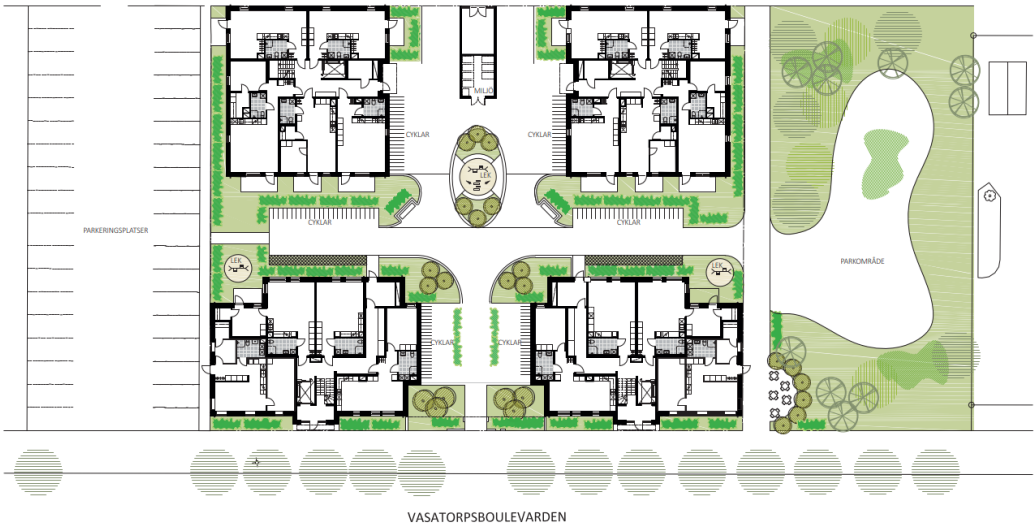

Figure 17. Layout of the construction project

3.1 BTES system

3.1.1 System operation

The subsystem of the Energy Centre, which includes the BTES and Ground Source Heat Pumps (GSHPs), is designed for both space heating and free cooling. This system enhances the electricity

production of the PVT panels by reducing their temperature, leveraging the stable and cool ground temperatures that remain unaffected by seasonal variations (see Figure 18).

Heat collected from the cooling unit and PVT panels can either drive the GSHPs to provide space heating and domestic hot water (DHW) to the buildings or be stored in the ground for use in the following winter season. During transitional seasons, different parts of the building may simultaneously require free cooling and space heating. In this mixed-mode operation, heat is rejected and supplied to the GSHPs for heating.

Although the connection between the DH network and the BTES system is currently non-operational due to regulatory restrictions, DH could be used to charge the BTES. This would reduce yearly primary energy consumption and achieve cost savings by lowering electricity use during winter. The primary advantage of incorporating DH is stabilizing the ground temperature by supplying heat during warmer months when DH prices are at their lowest, ultimately enhancing heat recovery over extended periods.

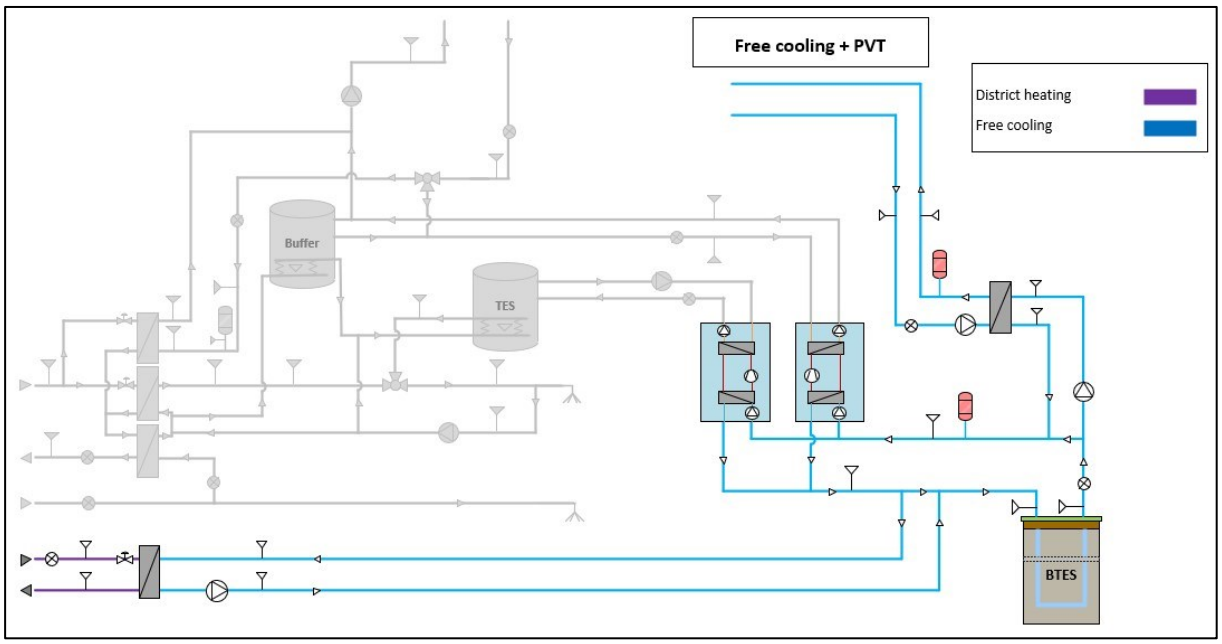

Figure 18. A subsystem of the Energy Centre including BTES and GSHPs for space heating and free cooling

3.1.2 BTES layout and schematic

The system concerned integrates a closed-loop shallow geothermal system. The nearly rectangular borehole field, measuring 22 by 24 meters, consists of 12 U-tube ground heat exchangers connected in parallel. Each borehole reaches a depth of 200 meters, with an average spacing of 9 meters between them.

A U-tube heat exchanger is installed within each borehole, facilitating efficient heat transfer between the ground and the fluid circulating in the system. This configuration is based on thorough field exploration and local hydrogeological data, which detail the material composition and depth of each geological layer.

The selection of the U-tube design is informed by the geological conditions of the site, allowing for optimal thermal exchange and minimizing resistance to fluid flow. The arrangement and depth of the boreholes are strategically planned to maximize the system's efficiency and ensure effective heat extraction and injection throughout the operational year. The integration of this closed-loop

system plays a vital role in the overall energy management strategy of the Tornet Energy Centre, enabling the harnessing of renewable geothermal energy to support heating and cooling needs.

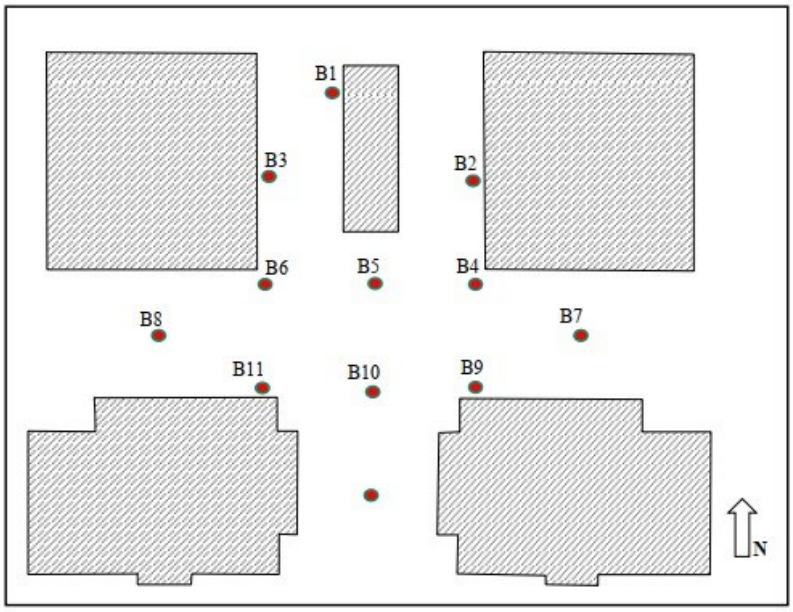

Figure 19. Layout of the borehole field in the Energy Centre

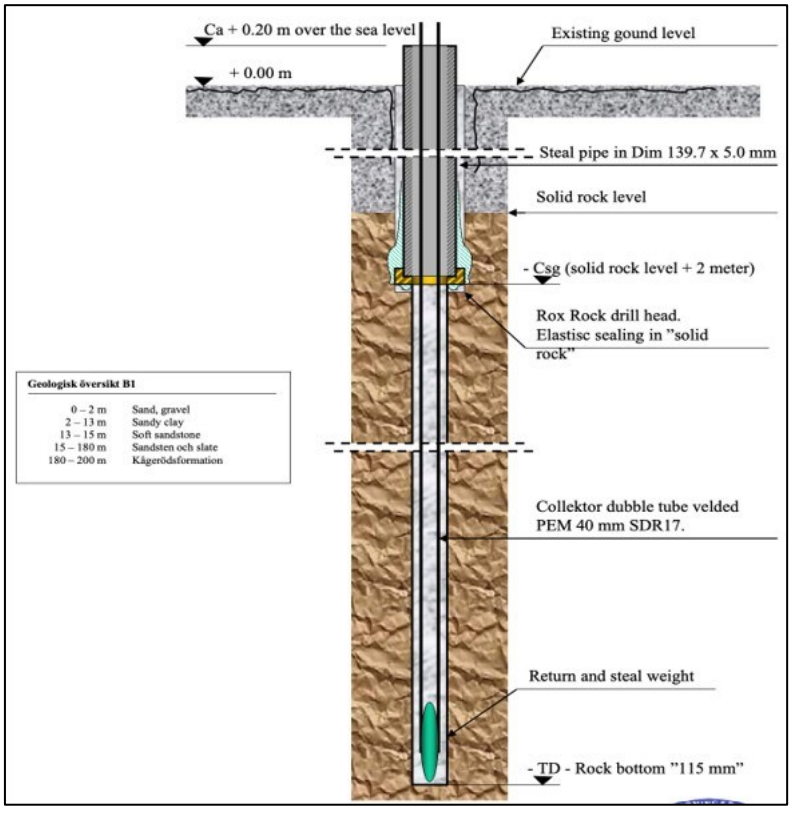

Figure 20. Schematic of the U-tube borehole heat exchanger and existing ground layers

3.2 BTES model

3.2.1 Key parameters, inputs and outputs

Accurate and rapid simulation of the BTES system's thermal response, in conjunction with other components, is essential for predicting subsystem performance. The in-house BTES model in TRNSYS simulates borehole heat exchangers uniformly distributed within a cylindrical volume, typically utilizing U-shaped pipes. The model accounts for heat transfer between the circulating fluid and the ground, incorporating both fluid-to-ground and U-tube interactions. The thermal process encompasses local, global, and steady-state effects, employing finite difference methods for local and global issues, alongside analytical methods for steady-state flow analysis.

Figure 19 presents a flowchart outlining the simulation and analysis steps of the BTES model. Key parameters include the geometry and thermal properties of the boreholes and U-tubes. Input variables consist of the inflow temperature (T_in,BTES), flow rate to the BTES, and ambient temperature. The model generates outputs such as the outflow temperature (T_out,BTES), average storage temperature, and various components of the energy balance, including heat loss, internal energy variation, and heat exchanged with the BTES.

To enhance model accuracy, the thermal properties of both the ground and grout were calibrated. Initially, the BTES performance was simulated and validated over two short periods using monitoring data. The model was then extended to simulate a 10-year period, evaluating performance with and without the integration of DH to assess its benefits. Given the lack of long-term input data, a refinement process was employed to augment the existing dataset. Ultimately, the thermal performance of the system was thoroughly evaluated and compared for both scenarios.

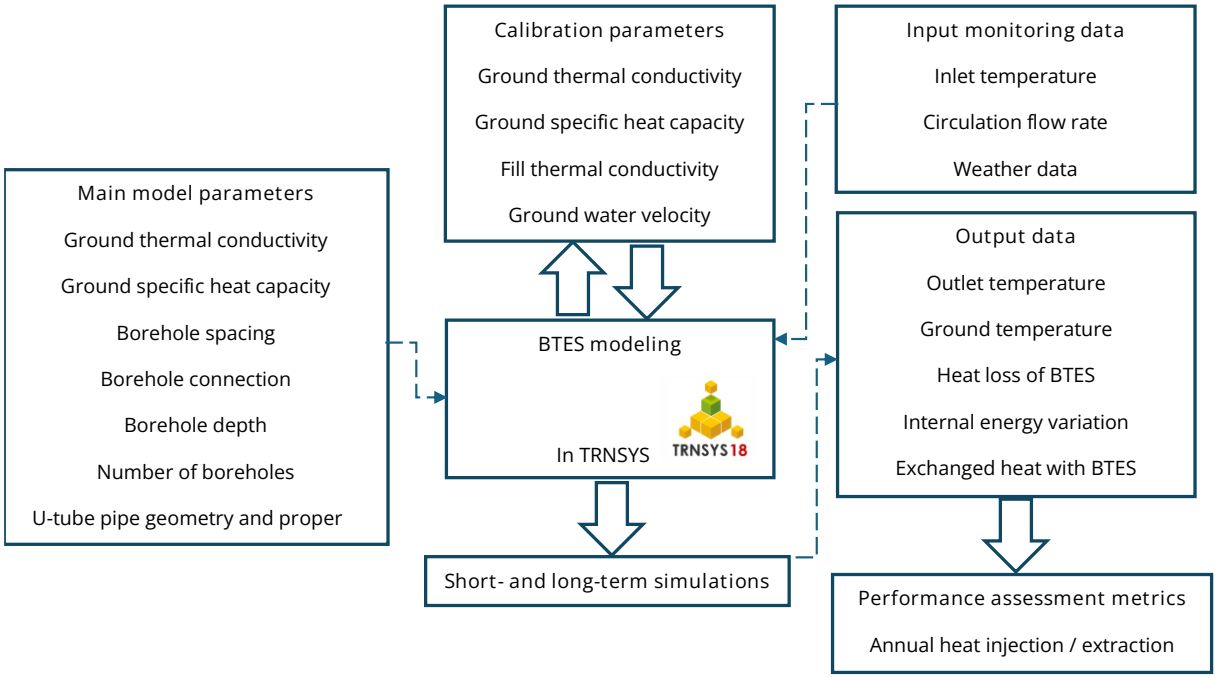

Figure 21. Flowchart of the BTES model simulation and analysis process

3.2.2 Model validation

The BTES model was validated by adjusting the calibration parameters using site specific monitoring data from two periods: September to October 2023 (Period 1) and November to January 2023-2024 (Period 2).

Period 1: charging phase

During Period 1, the BTES undergoes a charging process, with $T_{in,BTES}$ and $\dot{m}_{BTES}$ as shown in Figure 20. The inlet temperature (Inlet T) is displayed on the left axis and the mass flow rate (Inlet MFR) on the secondary axis. A clear daily pattern is observed, with $T_{in,BTES}$ ranging from 11.5°C to 18.0°C and $\dot{m}_{BTES}$ fluctuating between 7,000 and 26,000 kg/h.

During this period, the monitored outflow temperature (Outlet T, mon) ranges between 10°C and 12°C. The simulated outlet temperature (Outlet T, sim) is compared with the monitored data in Figure 21 for validation. Overall, the simulated $T_{out,BTES}$ aligns well with the monitored values, although some deviations are observed, particularly during spikes in $T_{in,BTES}$.

The uncertainty in the prediction of the simulated $T_{out,BTES}$ is assessed using the Root Mean Squared Error (RMSE) metric. The total RMSE for Period 1 is 0.3°C, with hourly RMSE values presented in Figure 22. As shown, the hourly RMSE remains below 1.1°C, except during a period of significant fluctuation in $T_{in,BTES}$ and $\dot{m}_{BTES}$ (Figure 20), where the RMSE briefly spikes to approximately 2.5°C.

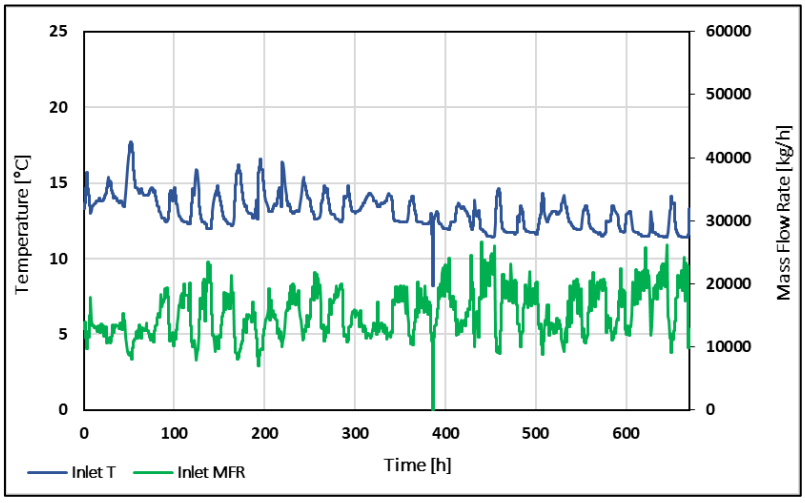

Figure 22. Inlet temperature and mass flow rate to BTES in Period 1

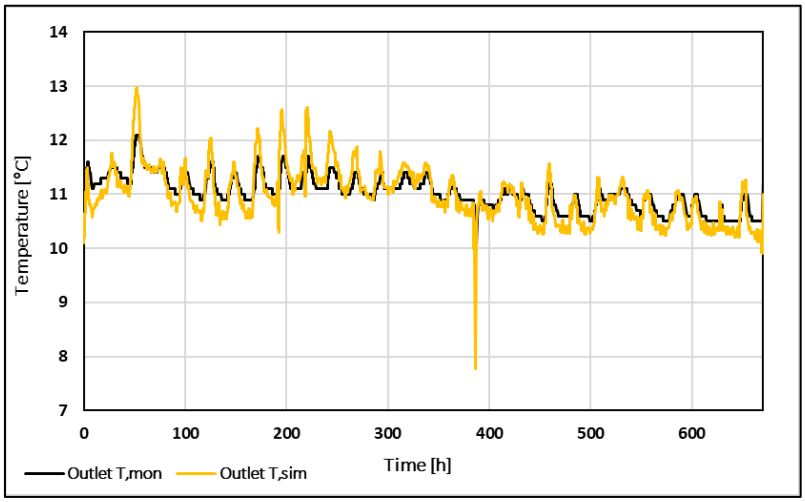

Figure 23. Comparison of simulated and monitored outlet temperatures from the BTES during Period 1

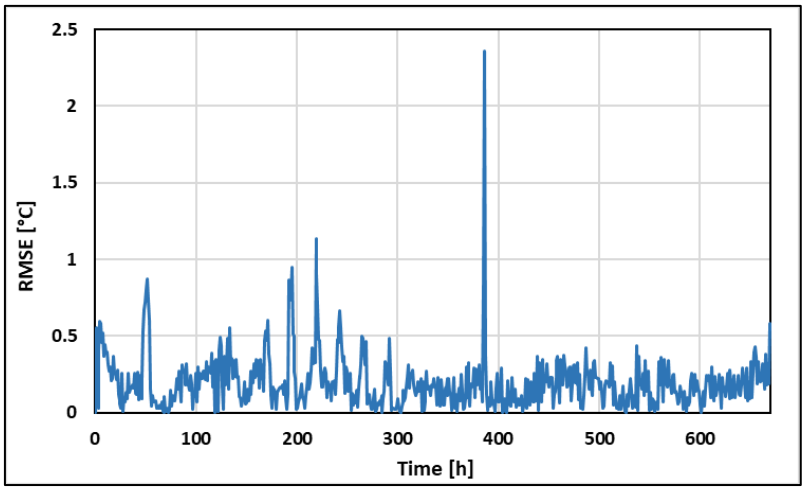

Figure 24. Hourly RMSE of outlet temperature from the BTES during period 1

Period 2: discharging phase

Figure 23 shows $T_{in,BTES}$ and $\dot{m}_{BTES}$ during Period 2, when the BTES is being unloaded. $T_{in,BTES}$ ranges from 0.3°C to 10.0°C, while $\dot{m}_{BTES}$ fluctuates between 900 and 45,000 kg/h.

The simulated and monitored $T_{out,BTES}$, along with the corresponding hourly RMSE for Period 2, are illustrated in Figures 24 and 25, respectively.

As in Period 1, the simulated $T_{out,BTES}$ closely matches the monitored data, with the hourly RMSE remaining below 0.6°C and a total RMSE of 0.3°C for the entire period.

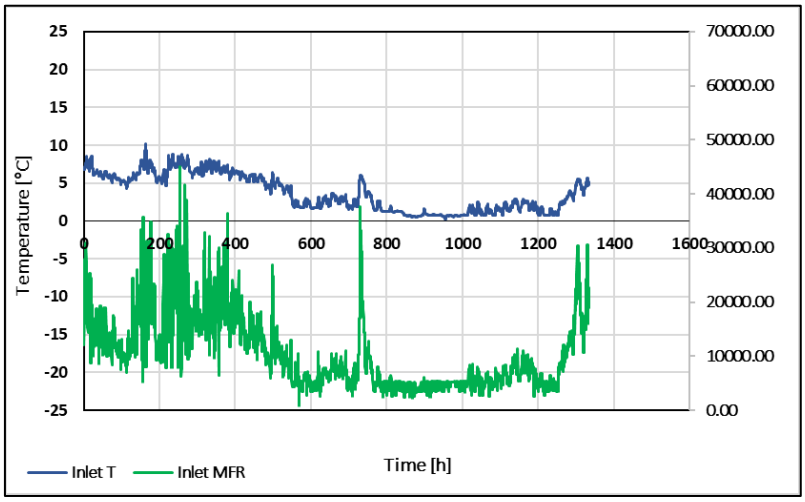

Figure 25. Inlet temperature and mass flow rate to BTES in Period 2

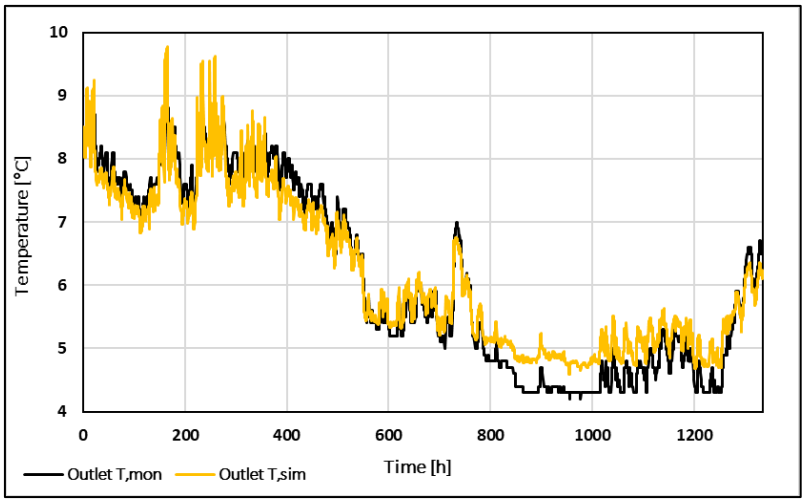

Figure 26. Comparison of simulated and monitored outlet temperatures from the BTES during Period 2

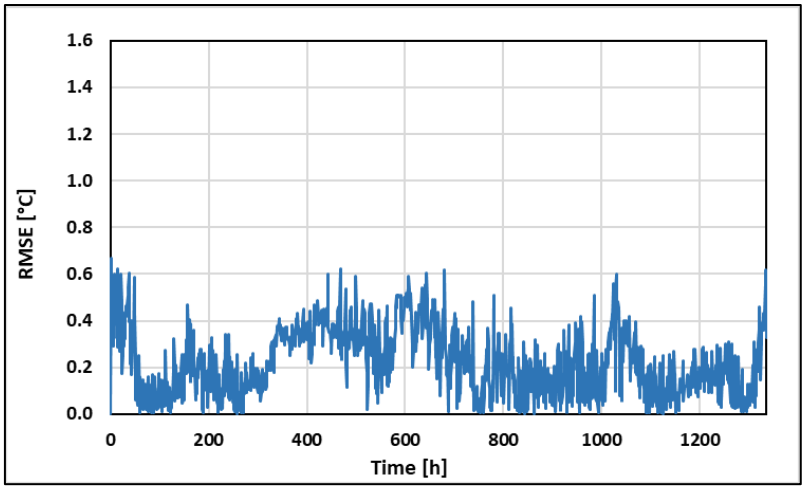

Figure 27. Hourly RMSE of outlet temperature from the BTES during period 2

3.3 One-year BTES simulation with and without DH

This section evaluates the performance of the BTES system over a one-year period, comparing scenarios with and without DH integration. While DH typically increases the outlet temperature of the BTES, its effectiveness depends on the heat injected from the PVT panels and the free cooling system. These additional heat sources can either enhance or interfere with the energy usage from DH.

To analyze these dynamics, we first compiled a year's worth of input data to simulate the BTES response. Since heat is rejected by both the free cooling system and the PVT panels, it is crucial to evaluate the thermal power profile influenced by the GSHP, free cooling, and PVT. The simulation results for both scenarios are then compared to determine DH's role in stabilizing the BTES and to assess its potential benefits within this specific configuration.

3.3.1 Input data refinement

Due to incomplete input data, the missing $T_{in,BTES}$ and $\dot{m}_{BTES}$ data were reconstructed by fitting models to the observed daily and seasonal variations. This approach replicated patterns, generating a continuous and realistic dataset for the entire year to ensure accurate model simulations.

Thermal power

Although the thermal power of the BTES is not a direct input to the model, generating its annual profile is crucial for understanding the total heat injected or extracted over the year. This profile reveals heat surplus or deficit within the BTES, influenced by the GSHPs, free cooling, and PVT panels. Accurately assessing this balance is key to optimizing system performance and ensuring the long-term stability of the BTES. Figure 28 presents the current monitoring of the thermal power exchanged with the BTES. The data gaps prevent an accurate calculation of the annual heat surplus or deficit.

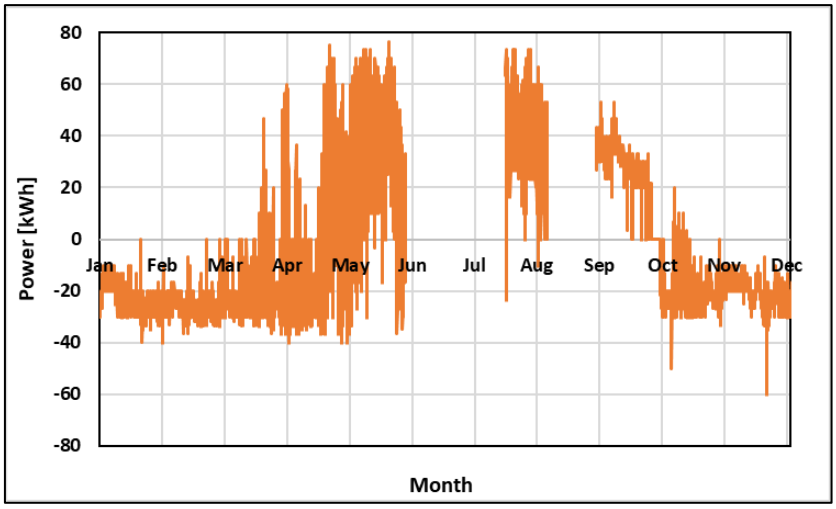

Figure 28. Actual exchanged thermal power with the BTES

Rather than using interpolation techniques to fill the gaps, it was decided to use simulation results as boundary conditions. The simulation starts with the district heating temperature profile and the load profiles (for domestic hot water, space heating, space cooling, and PVT production), which have been validated using monitoring data.

DH supply temperature

Figure 29 displays the actual DH supply temperature in orange and the reconstructed temperature in blue. The reconstructed temperature ranges from 70°C in summer to 90°C in winter and it is based on a sinusoidal curve.

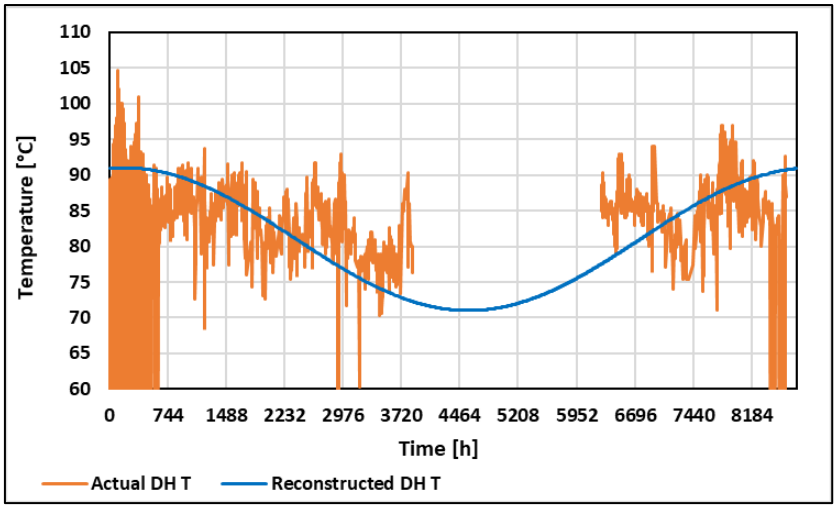

Figure 29. Actual vs. reconstructed supply temperature of DH

DHW load

Figure 30 shows the domestic hot water hourly thermal energy profile acquired, from the 11th of October to the 31st of October. This profile exhibits a predictable daily pattern, with stochastic behavior superimposed on it. The latter can be assessed by filtering the daily sinusoidal pattern from the signal acquired and assessing the probability density function of the remaining timeseries. Combining the daily pattern with hourly variations, aligned with the assessed stochastic deviations, allows for filling the gaps, as illustrated in Figure 31. This technique was used to fill all the gaps and define an hourly domestic hot water profile for an entire year.

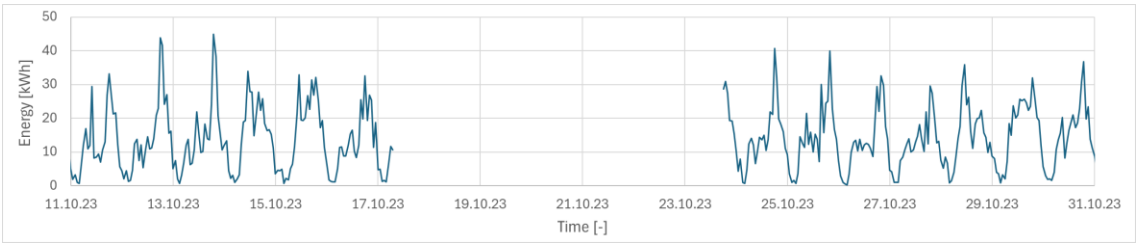

Figure 30. Domestic hot water hourly thermal energy profile from monitoring data (11th October 2023 – 31st October 2023)

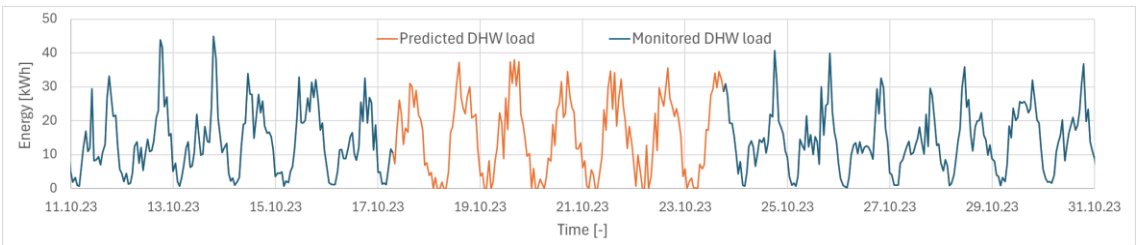

Figure 31. Domestic hot water hourly thermal energy profile from monitoring data with prediction to fill the gaps (11th October 2023 – 31st October 2023)

SH loads

The space heating load profile was established by linking the hourly load to the heating degree hours (base 20°C) for the corresponding time interval. Historical temperature records for Helsingborg were utilized to determine the heating degree hours assigned to each monitored space heating load value. Figure 32 illustrates the correlation between heating degree hours and the hourly space heating load. The data was then regressed to derive an equation that defines the space heating load as a function of the outdoor air temperature, as shown in Figure 33.

Using this prediction, the mean bias error is -0.79 kWh, and the normalized root mean squared error is 8%.

In the simulations presented in the following text, the weather data is sourced from Meteonorm, resulting in a space heating profile that slightly differs from the monitored space heating profile, while being representative of an average heating seasons in Helsingborg.

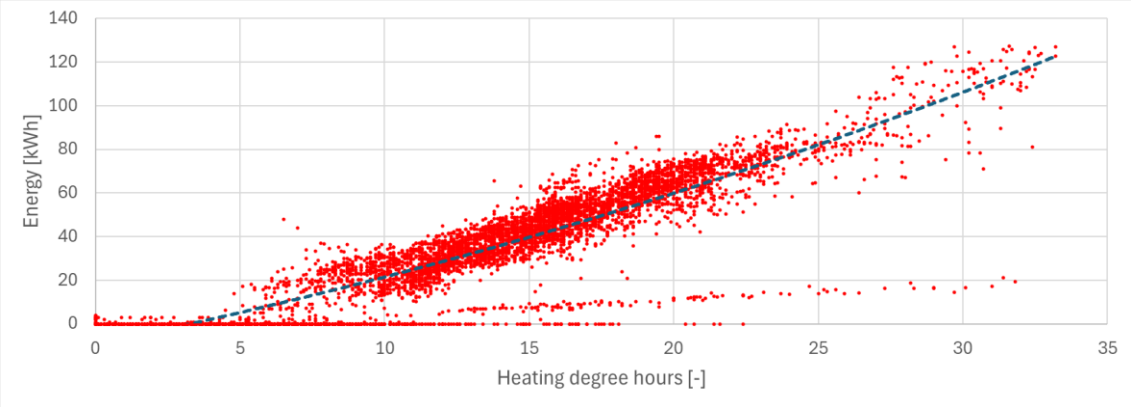

Figure 32. Correlation between the heating degree hours and the hourly space heating load

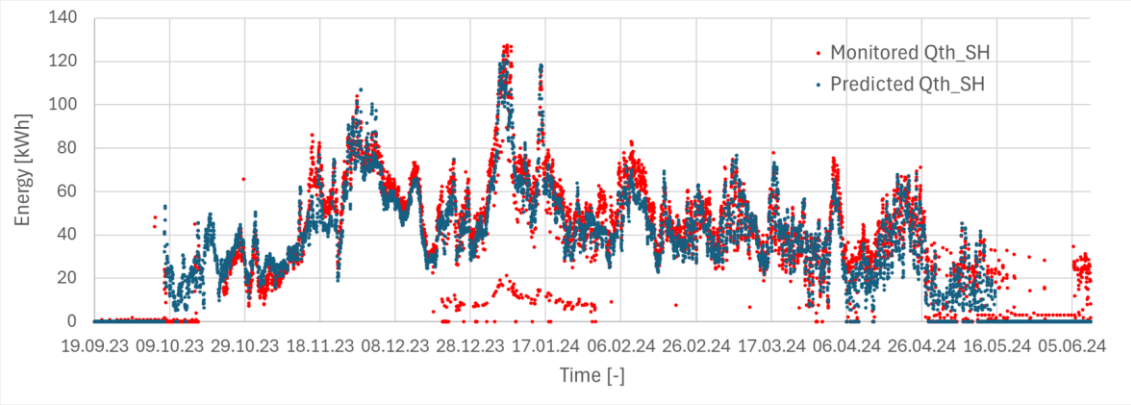

Figure 33. Monitored and predicted space heating load for the 2023-2024 heating season

SC loads

To define the space cooling load profile the same approach was used: the space cooling load is associated to the hourly cooling degree hours (base 10°C) for the same time interval.

The calculated mean bias error is -3.37 kWh, and the normalized root mean squared error is 12%. Similar to space heating, in the simulations reported, the weather data is sourced from Meteonorm, resulting in a space cooling profile that slightly differs from the monitored space cooling profile.

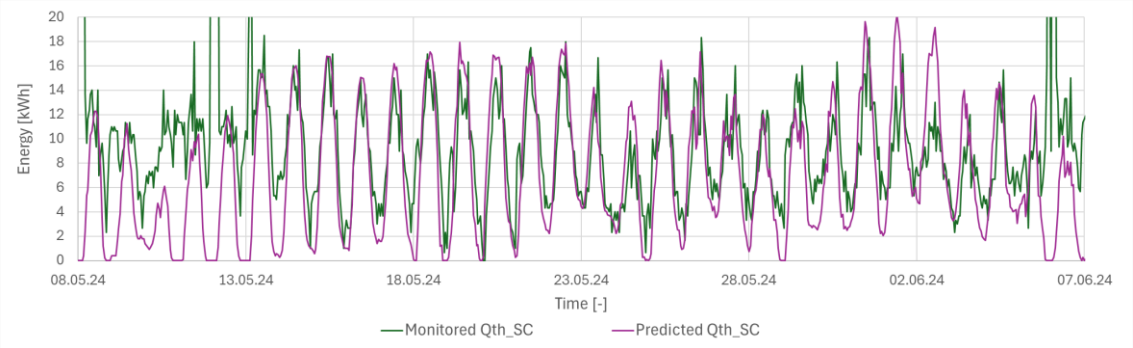

Figure 34. Monitored and predicted space cooling load (8th May 2024 – 8th June 2024)

PVT production

Finally, a similar technique was employed to determine the production of the PVT system. In this instance, the load was compared against global horizontal irradiation rather than temperature. Using this prediction, the mean bias error is 0.59 kWh, and the normalized root mean squared error is 4%.

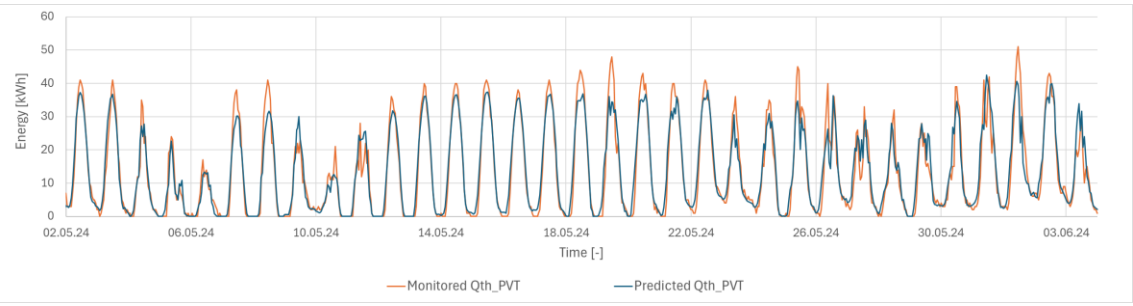

Figure 35. Monitored and predicted PVT production (2nd May 2024 – 4th June 2024)

BTES loads

The above temperature and load profiles were used in the energy system simulation, allowing to define the hourly energy drawn from or fed to the BTES. Figure 36 shows the monitored and simulated hourly energy that is extracted from or injected to the BTES.

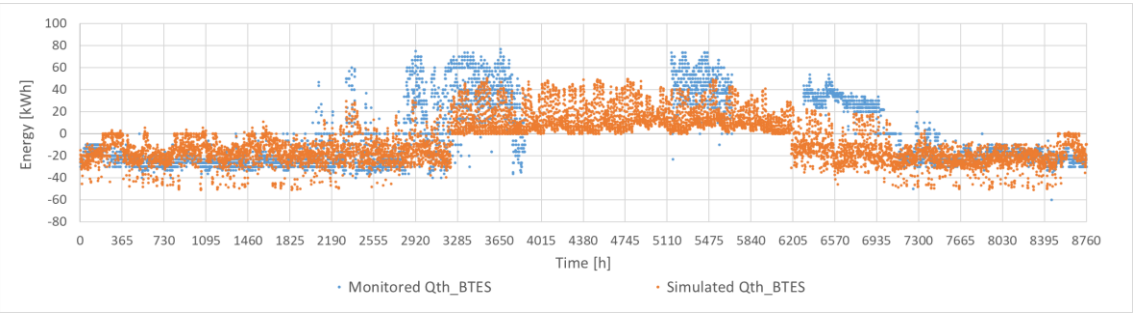

Figure 36. Monitored and simulated hourly thermal energy of the BTES

It can be noticed that until May and after September the two profiles are very similar. The difference between the two profiles is mainly caused by the fact that the monitored data represent a specific year (from September 2023 to June 2024), while the simulated data refer to a characteristic year.

During the heating season the energy extracted from the BTES to run the heat pump is higher than the energy fed to the BTES through PVT production. In the simulation we shut off the heat pump after mid-May, as there is no space heating load since. Additionally, from April onwards, the district heating price decreases, making it preferable to cover the domestic hot water load with district heating instead of the heat pump.

Monitored and simulated energies are different mainly during the cooling season, where the monitored heat (when data are available) fet to the BTES is slightly higher than the simulated one.

3.3.2 Simulation results without DH integration

Figure 37 shows the hourly simulated profiles of the BTES outlet temperature (left axis) and grond average temperature (right axis) over a year, in the base case scenario without DH integration.

As expected, the average BTES temperature at the end on the year is lower than the initial temperature. As this drifts continues over time, the HP's COP also shrinks, leading to both increased electricity consumption and energy drawn from the DH, due to the HP being unable to cover peak loads.

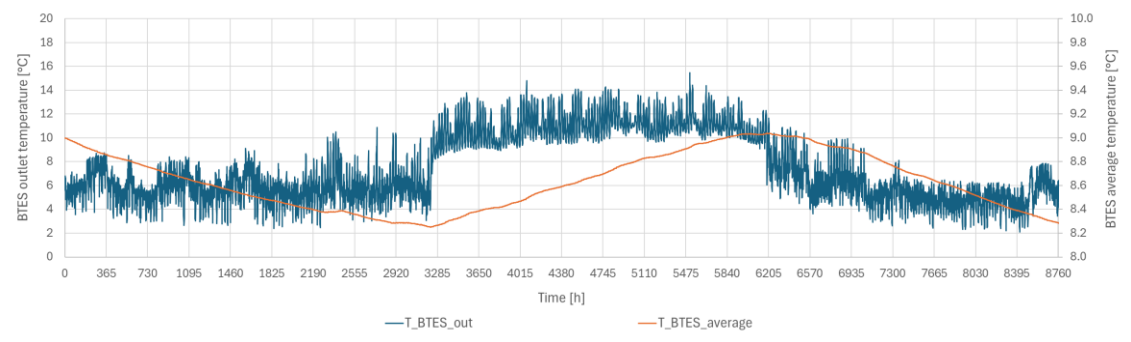

Figure 37. Hourly profiles of BTES outlet temperature (blue) and BTES average temperature (orange) over a year without DH integration

3.3.3 Simulation results with DH integration

To mitigate the effect, heat can be taken from district heating in summer, when energy cost is low and clearly the DH primary energy mix is the lowest as fossil fueled CHP units are surely off. Nonetheless, some boundary conditions need to be imposed. Sure, here's a rephrased version: to enable space cooling, the outlet temperature of the BTES must not exceed 15°C. The heat exchanger (HX) between the district heating (DH) and the BTES circuit has a nominal capacity of 50 kW. The control logic for charging the BTES with DH should ensure that the draw does not cause the BTES outlet temperature to surpass this limit.

If the BTES is not charged with DH, the difference between the extracted and injected energy is 56.7MWh. Theerefore, considering losses, the target energy to inject in the BTES is approximately 60MWh per year. Considering a maximum thermal capacity of 50kW, the BTES should be charged for 1200 hours to reach the target energy, corresponding to roughly 2 full operation months. To limit the thermal losses of the BTES it is convenient to inject heat in late summer (August and September) before the heating season starts and the DH price is low (Figure 38).

Figure 39 shows the hourly simulated profiles of BTES outlet temperature and BTES average temperature over a year with DH integration from August 1st to September 15th.

Because the limitation on the BTES outlet temperature (15°C) it is not always possible to feed 50kW in the BTES. Therefore, the total energy recovered amounts to only 36MWh, and the ground temperature at the end of the year is anyhow lower than the intial. Nevertheless, considering an initial average temperature of 9°C, if the BTES is charged during Summer, the average temperature at the end of the year is 8.7°C instead of 8.3°C, as in the base case scenario.

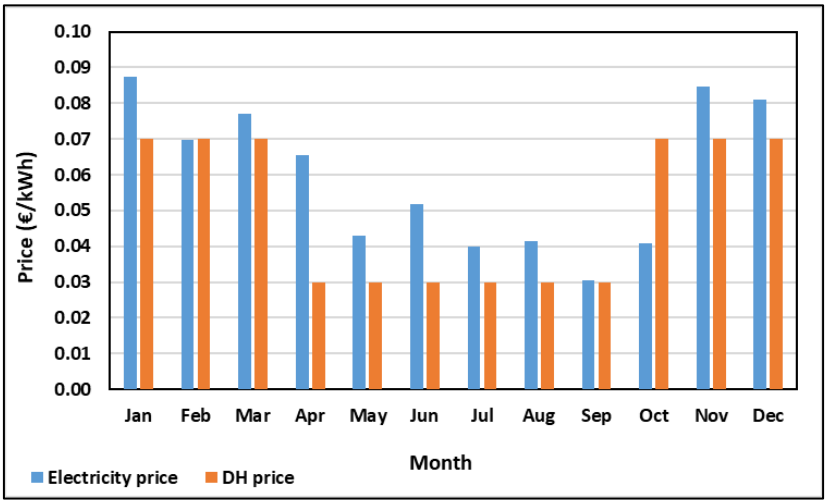

Figure 38. Monthly Electricity and DH prices

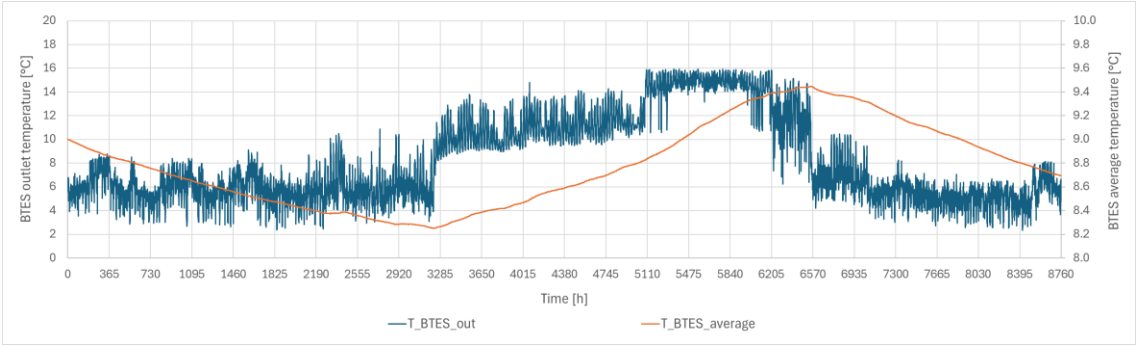

Figure 39. Hourly profiles of BTES outlet temperature (blue) and BTES average temperature (orange) over a year with DH integration (50kW from 1st of August to 15th of September)

3.4 10-year BTES simulation with and without DH

While the one-year simulation shows only minor difference in final BTES average temperature for the two scenarios, extending the analysis to ten years offers deeper insights into its cumulative impact. The boundary conditions and the corresponding temperature and load profiles describer in Subsection 3.3.1, were extended to simulate a 10 years of operation.

3.4.1 Base case scenario without DH integration

Figure 40 shows the hourly simulated profiles of BTES outlet temperature (left axis) and groud average temperature (right axis) over 10 years of operation, without DH integration. The average BTES temperature continues to trend downward throughout the entire simulated period. After 10 years, the average BTES temperature reaches 6.1°C, indicating a drop of nearly 3°C over the decade.

Over the same period, the total energy cost rises by approximately €1,100, which is a 6% increase from the initial cost. Specifically, the electricity cost increases by 5.5% (€305), and the district heating (DH) cost rises by 7.3% (€790). Figure 41 reports on such annual energy cost, split in electricity and DH cost.

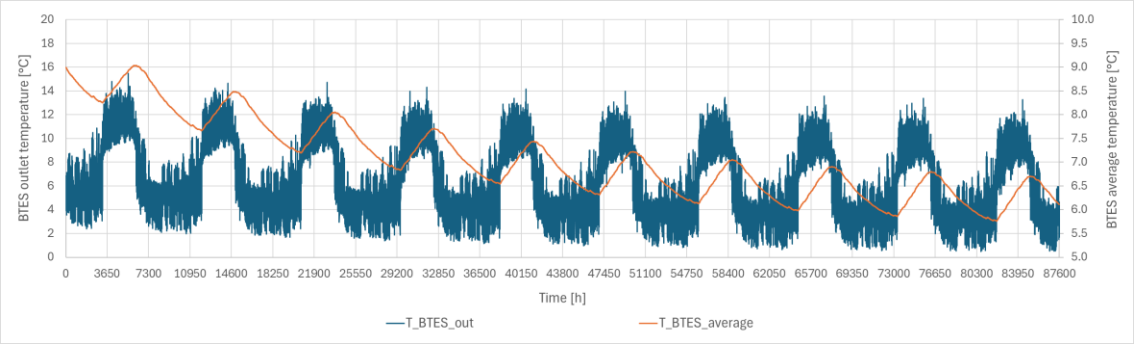

Figure 40. Hourly profiles of BTES outlet temperature (blue) and BTES average temperature (orange) over 10 years without DH integration

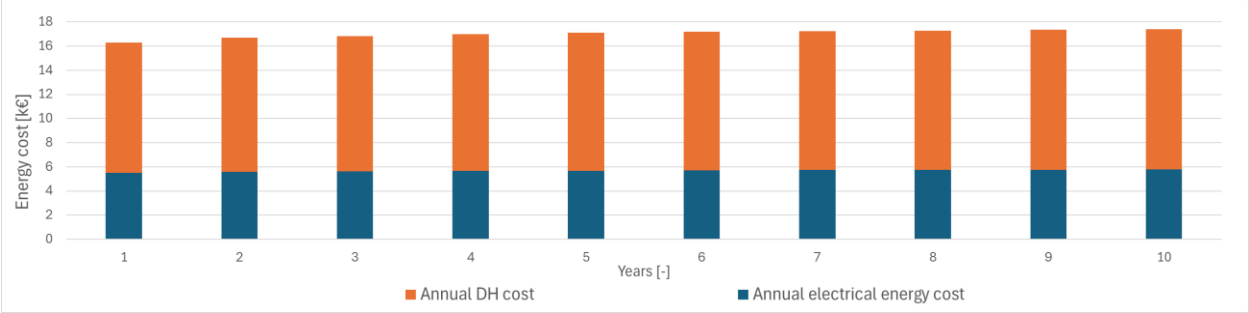

Figure 41. Variation of energy cost of the system over 10 years

3.4.2 Advanced scenario with DH integration

Figure 42 illustrates the hourly simulated profiles of the BTES outlet temperature (left axis) and the average BTES temperature (right axis) over 10 years of DH integration, from August 1st to September 15th. After 10 years, the temperature is 8.3°C, indicating a drop of only 0.7°C over the decade.

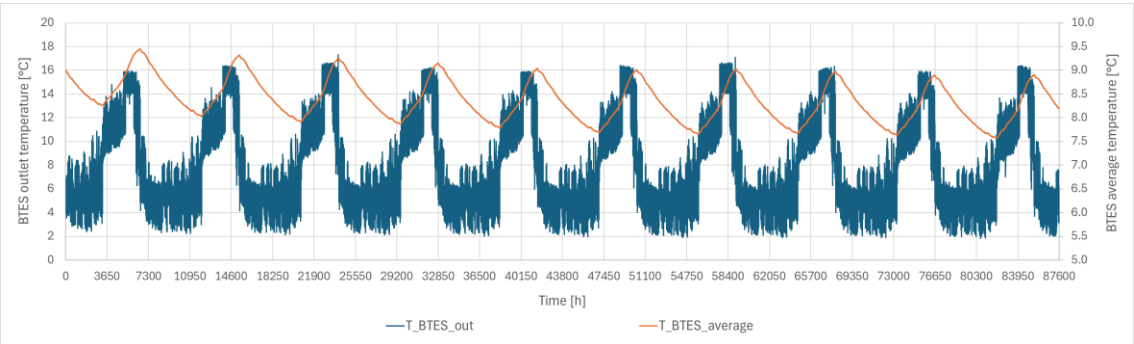

Figure 42. Hourly profiles of BTES outlet temperature (blue) and BTES average temperature (orange) over 10 years with DH integration (50kW from 1st of August to 15th of September)

Under these conditions, charging the BTES during summer saves 25 MWh of electrical energy over 10 years. However, it necessitates feed 390 MWh of energy from DH into the BTES during summer. According to the prices in Figure 38, this results in an operational cost increase of €9,303.60 over 10 years. Only with DH enrgy costs from August to September down to €7.4/MWh (instead of €30/MWh), summer BTES charging would be more economically viable.

3.5 Conclusions

The BTES system stores and manages thermal energy for space heating, domestic hot water, and space cooling applications. Understanding the long-term behavior of the BTES is crucial to identify potential issues over time. Due to insufficient monitoring data to characterize the annual and long-term behavior of the BTES, this analysis was based on simulation data. To align with actual system operation, a set of boundary conditions (DH temperature profile, domestic hot water, space heating and cooling demand profiles, and PVT production profile) was established using monitoring data. These conditions were then applied in a simulation model that includes the energy system components and control strategy.

The simulation results allowed for the analysis of both short-term and long-term BTES behavior, focusing on two scenarios. In the first scenario, the BTES and the rest of the energy system operate in a manner that emulates real behavior. In the second scenario, additional energy is injected into the BTES through district heating integration.

- Performance of the current system: The simulation results indicate that with the current control strategy, the energy extracted from the BTES to run the heat pump during the heating season exceeds the energy injected into the BTES via the PVT system and space cooling. The annual internal energy variation is approximately -60 MWh per year, resulting in a ground temperature drop of about 3°C over 10 years. This temperature decrease affects the BTES outlet water temperature, leading to increased heat pump electrical consumption. Additionally, the temperature drop at the evaporator reduces the heat pump's thermal capacity, necessitating more district heating to cover domestic hot water and space heating demands during the heating season. After 10 years, the total energy cost increases by nearly €1,100, corresponding to a 6% rise in initial expenses.
- Performance with DH integration: To mitigate the drop in BTES average and outlet temperature, heat can be injected into the BTES through district heating. Since feeding the BTES with 50 kW of thermal power can sometimes cause its outlet temperature to exceed the space cooling limit of 15°C, the actual energy that can be stored in the BTES is 35.7 MWh. Over 10 years, this results in a temperature decrease of only 0.7°C. This operation saves 25 MWh of electricity over 10 years at the cost of an additional 390 MWh from district heating.

3.5.1 Lessons learned

- Challenges in data collection: Real-time data on BTES system performance is crucial for assessing long-term thermal balance, highlighting the need for future monitoring to detect imbalances early. A significant challenge during the project was incomplete input monitoring data. The lack of continuous data, especially for key parameters like inlet temperature and mass flow rates, required extensive data refinement and reconstruction. The robustness and reliability of monitoring systems should be continuously checked.
- Challenges and potential in DH integration: Integrating DH into the BTES while considering actual system utilization presents operational constraints. The strategy for reintegrating this

energy must be meticulously defined and calibrated to be economically, energetically, and environmentally feasible. Alternative control strategies to optimize the operation of both systems should be explored. Lowering the charging power, extending the charging period, and optimizing the control strategy could positively impact system performance. For economic feasibility, the price of district heating during summer should be €7.4/MWh instead of €30/MWh. Primary energy and CO2 emissions savings at the energy system level should be evaluated to justify such a reduction.

4 Overall Conclusions

The comprehensive analysis of the Gardanne mine shaft and Helsingborg BTES system underscores the potential and challenges of using long-term thermal energy storage solutions in district heating and cooling networks.

The Gardanne mine shaft, with its significant water volume and depth, presents a viable option for seasonal thermal energy storage. However, the study revealed that external factors, such as groundwater infiltration and the influence of neighbouring wells, significantly impact its thermal behaviour. These findings emphasise the need for a thorough understanding of site-specific conditions and continuous monitoring to optimise storage performance.

The BTES system in Helsingborg demonstrates the effectiveness of integrating geothermal energy with district heating and cooling. Introducing district heating to charge the BTES during summer mitigates the temperature drop. This approach saves 25 MWh of electricity but requires an additional 390 MWh of district heating energy, highlighting the trade-off between energy sources and costs. The economic feasibility of this strategy depends on the district heating price, which should be significantly lower during summer months to justify the investment, substantiated by eventual environmental benefits at the energy system level.

Ground data analysis and numerical simulations are key to accounting for the dynamic interactions between the seasonal energy storage and its surrounding environment. Tailored operational strategies and continuous monitoring maximise the benefits of long-term thermal energy storage systems. These measures should be implemented from the very beginning of the planning phase and throughout the operation of the seasonal thermal storages.

5 References

[1] Zhang C, Lu X, Guo Y, Xu C, Peng D. Thermal performance of two-independent-circuit borehole heat exchanger in solar-assisted ground source heat pump system. Renewable Energy 2024;230:120860. https://doi.org/10.1016/j.renene.2024.120860.

[2] Yuan T, Ding Y, Zhang Q, Zhu N, Yang K, He Q. Thermodynamic and economic analysis for ground-source heat pump system coupled with borehole free cooling. Energy and Buildings 2017;155:185–97. https://doi.org/10.1016/j.enbuild.2017.09.018.

[3] Wu W, You T, Wang B, Shi W, Li X. Evaluation of ground source absorption heat pumps combined with borehole free cooling. Energy Conversion and Management 2014;79:334–43. https://doi.org/10.1016/j.enconman.2013.11.045.